A Multi-objective Optimization for the Power Management of Shipboard Zonal DC Microgrids

Andrea Alessia Tavagnutti
Dept. of Engineering and Architecture
University of Trieste
Trieste, Italy
andreaalessia.tavagnutti@phd.units.it

Daniele Bosich
Dept. of Engineering and Architecture
University of Trieste
Trieste, Italy
dbosich@units.it

Andrea Vicenzutti
Dept. of Engineering and Architecture
University of Trieste
Trieste, Italy
avicenzutti@units.it

Valentino Pediroda
Dept. of Engineering and Architecture
University of Trieste
Trieste, Italy
pediroda@units.it

Giorgio Sulligoi
Dept. of Engineering and Architecture
University of Trieste
Trieste, Italy
gsulligoi@units.it

***Abstract*—In the marine industry, flexibility on load supply and efficiency on prime movers are the key elements to develop advanced shipboard systems. To achieve these outcomes, the DC zonal distribution is preferable, as it can enable the most suitable power transfer from sources and storage to loads. In these systems, the high-level control logics are integrated in the Power Management System (PMS), which coordinates the power converters to guarantee the ship mission. The paper is aimed at proposing an optimization algorithm to lead the PMS actions on the controlled DC system. By setting the power setpoints on the interface converters, the optimized PMS can ensure the best use of prime movers, while preserving the duration of energy storage support. By switching from single objective to multi-objective, the optimization can purse the best operating points both in single and in separated buses configuration, thus enhancing the use of energy onboard and the autonomy along the ship route.**

Keywords—multi-objective, optimization, ZEDS, DC microgrid, efficiency, autonomy, ship.

I. Introduction

As in the whole transportation sector, also the maritime industry is facing an extensive electrification process. In this regard, the All Electric Ships (AES) can indeed guarantee a high degree of flexibility and an enhanced ship efficiency [1], paving the way for innovative power system architectures. Among them, the zonal topology based on DC distribution is the one to be adopted when high performance is mandatory [2], as in naval vessels. In such complex DC systems, the operations are ensured only in presence of an optimized coordination of multiple power electronics converters [3]. These intelligent interfaces enable the full controllability of DC grid, while making possible the interface to different types of sources/storages, as well as the supply of different power loads. As usual practice in microgrids, a hierarchical control is also exploited in shipboard DC grids [4], while the control concept is further improved when moving onto Zonal Electrical Distributions System (ZEDS) [5]. The overall coordination and management of the power distribution is conventionally assigned to a Power Management System (PMS), integrating high-level control logic to define setpoints and commands to be sent to the field and zonal controllers. Being the ship an isolated system with limited resources, an optimized management of sources and storage can drastically improve the ships operability, autonomy, and lifetime [6]. In this paper an optimized management of an exemplifying two-buses ZEDS is chosen as case of study. To show the flexibility of the zonal architecture, the performed test is about the ship entry maneuver in a port, where the two buses are to be operated independently for safety reasons. An optimization algorithm is integrated into the shipboard PMS to set the control references on converters for both normal and split-buses configurations. Since the powering of a load zone is shared between the two buses, the optimization algorithm is properly configured to effectively operate also when port-starboard buses are separated.

II. Shipboard Zonal DC Microgrid

This paper wants to discuss an optimized management to be integrated into the PMS of zonal DC shipboard microgrids. This optimization is aimed at ensuring the highest efficiency operating point on diesel engines, while preserving a convenient State of Charge (SOC) on the onboard batteries. This Section presents the zonal DC grid on which perform the optimization.

A. Optimization on zonal DC systems

The zonal DC distributions are globally recognized as best effective when advanced flexibility in managing high-performance power converters is required [7]. In such DC systems, the large-bandwidth interfaces are controlled to dynamically transfer the power to the loads, thus ensuring the ship mission [8]. In these controlled grids, energy storage plays a crucial role. Battery storage systems are usually placed to assist the low-dynamics diesel engines to allow fast reallocation of the onboard power [9]. To feed a large load power quite-instantaneously, the very initial supply comes from the charged batteries. Then, the supply is entirely covered by diesel engines, once they conclude their power-up ramp. When the DC grid is powered by both diesel engine and batteries, a combined optimization is necessary to ensure a wise power management. The study on this paper wants to guarantee the diesel engines' operation in their highest efficiency point, while leaving the batteries SOCs as constraints (i.e., admissible area). In Authors opinion, this approach is the most convenient trade-off between final result, optimization complexity, and operating time.

Co-funded by the European Union, Horizon Europe Program - V-ACCESS Project; Grant agreement ID: 101096831.
"Views and opinions expressed are however those of the authors only and do not necessarily reflect those of the European Union. Neither the European Union nor the granting authority can be held responsible for them".

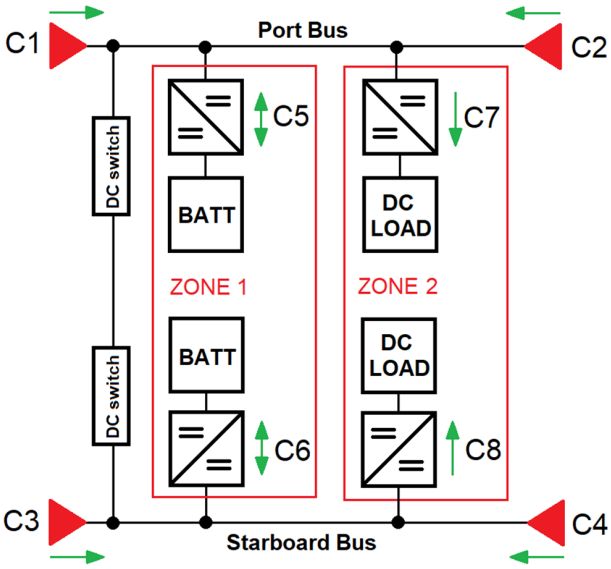

Fig. 1. Zonal DC shipboard microgrid.

B. Zonal DC microgrid

The paper develops a strategy to optimize the operation of the zonal DC microgrid in Fig. 1. The latter is an onboard distribution grid, having two zones (red boxes) and four power-input stages (triangles). The green arrows express a typical power flow. Each triangle is the cascade of three elements (i.e., diesel generator DG, diode rectifier, and DC-DC boost converter). The system has two DC switches to make available its decoupled operation as two independent grids. This work considers both configurations, thus envisaging a single bus or two buses. Although the zones number is limited to two, the same approach proposed afterwards can be replayed/extended to ZEDS with more zones. As shown in the Tab. I data, the four red inputs (i.e., C1-C4 as interface converters) can provide a total power of 6 MW to the loads, which is sufficient to feed the two embarked loads, each equal to 3 MW (i.e., rated power of C7 and C8). The bus voltage is 1.5 kV, whereas the load voltage at the output of C7-C8 is lower, 1.3 kV. Each battery provides 1 MWh, while the output rated voltage is 1.2 kV. The power sizing of the batteries' converters is set to supply transient power only (i.e., the total load demand at steady state is equal to total power from red inputs). To simplify the scheme, the LC filtering stages on each converter (i.e., power quality issue) are not drawn.

C. Control of power electronics interfaces

The C1-C4 are DC-DC boost converters, used to the external power input. Then, the C5-C6 elements provide a bidirectional operation. The latter are used as boost converters, with the batteries supporting and regulating the bus voltage. On the loads side, the two buck converters C7-C8 provide the step-down function. The C1-C4 converters are current controlled, where a power reference from the PMS is translated into a current setpoint. The bus voltage is droop-controlled by C5-C6 batteries converters, while the loads are voltage controlled by C7-C8. A central controller implements the PMS function, by sending the setpoint to the zonal controllers to manage loads, sources and energy storages. The optimization algorithm acts on the PMS to maximize efficiency and range of the controlled ship.

TABLE I. Design data of interface power converters.

	C1	*C2*	*C3*	*C4*	*C5*	*C6*	*C7*	*C8*
P_n [MW]	2.0	1.5	1.0	1.5	1.0	1.0	3.0	3.0
V_{in} [kV]	1.0	1.0	1.0	1.0	1.2	1.2	1.5	1.5
V_{out} [kV]	1.5	1.5	1.5	1.5	1.5	1.5	1.3	1.3
D_{k0} [·]	0.75	0.50	0.75	0.50	0.75	0.50	0.75	0.50
I_{k0} [A]	323	240	323	240	323	240	323	240

D. Optimal working condition

To guarantee maximum efficiency, the DGs should work around their optimal operating point. This results in a reduced fuel consumption and less harmful emissions. At the same time, the batteries are to be maintained inside a certain SOC range, to avoid excessive degradation and for stability reasons. Being them assigned to bus voltage control, if their SOC (thus their voltage) decreases to a certain level their regulation capability is compromised, which may lead to unstable behaviors. To reach the optimal working condition, the output powers of converters represent the variables, while converters/DGs rated power and batteries SOCs behave as constraints.

III. Operating Point Optimization

The shipboard DC microgrid operation is supervised by a PMS centralized controller. This PMS is also responsible for the optimization of the power distribution operating point. The algorithm is performed every 10 minutes, in order to guarantee safe operation while reducing fuel consumption and batteries degradation. The algorithm takes into account the configuration of the DC system, the expected load variations, and the intrinsic limitations of power distribution.

A. Optimization engine

To extend the correspondence to reality, the optimization engine is real-time adapted to the actual configuration of the DC system. Thus, it performs a single objective optimization when the DC switches are closed, while moving onto a two objective optimization when the busbar connector is open. When the two buses are connected, all the converters work together, exchanging power between the buses through the busbar connector. In this configuration, it is possible to consider the DC grid as a whole, thus defining a single objective function. The goal is to find the power setpoints P_i allowing the DGs to work at their maximum efficiency (nearly 80% of their rated power). To perform this single objective optimization, the selected objective function $f(P_i)$ in (1) takes into account the distance from the optimal power of the four generating converters P_i^*.

$$\min f(P_i) = \min[\sum_{i=1}^{4} (P_i^* - P_i)^2] \quad (1)$$

Differently, when the zonal DC grid works with the busbar connector open, the problem become more complex, being present two subsystems operating simultaneously. These subsystems are not completely independent from one another, since they share the zones of batteries and loads. This aspect reflects on the constraints. When the busbar is open, the PMS is required to perform a two-objective optimization, as in (2)-(3).

$$f_1(P_i) = (P_1^* - P_1)^2 + (P_2^* - P_2)^2 \quad (2)$$

$$f_2(P_i) = (P_3^* - P_3)^2 + (P_4^* - P_4)^2 \quad (3)$$

B. Constraints

To perform the optimization, the algorithm takes into account a set of constraints, with the following set of equalities and inequalities. The first equation to be included is the electrical power balance of the DC grid, as in (4) for the single objective optimization. While, for the two-objective optimization (i.e., two independent buses), (4) is divided in two equations, considering the two buses independently. Then, the power equilibrium sets (5), where the power outputs from converters C7-C8 (i.e., x_7=P_7 and x_8=P_8) has to equal the requested load power P_{load}. Indeed, the two loads are treated as a single one, being the power converters capable to shift the load from one bus to another thanks to the zonal architecture. The batteries are fundamental components in the DC grid, being assigned of the bus voltage regulation. In this regard, the condition (6) on their SOC is mandatory. Finally, the last three inequalities relate to the acceptable range of each variable. In detail, (7)-(9) take into account the DG rated power (i.e., P_{iR}), the maximum output/input power of batteries (i.e. $P_{maxbatt}$) and the maximum load power (i.e., $P_{maxload}$). Additional remarks can be made on $P_{maxbatt}$, chosen by the PMS to avoid very fast charge/discharge on the battery. In this case, the chosen value is 400 kW, while enabling additional modifications during the ship operation to adapt it to the power system needs. Thanks to the 6 constraints, the optimization engine can identify the optimal operating points. Being in accordance with the constraints, the latter are acceptable for both power grid and its components.

$$\sum_{i=1}^{8} P_i = 0 \quad (4)$$

$$x_7 + x_8 = P_{load} \quad (5)$$

$$30\% \leq SOC \leq 80\% \quad (6)$$

$$0 \leq x_i \leq P_{iR} \qquad i = 1,..,4 \quad (7)$$

$$-P_{maxbatt} \leq x_i \leq P_{maxbatt} \qquad i = 5,6 \quad (8)$$

$$-P_{maxload} \leq x_i \leq 0 \qquad i = 7,8 \quad (9)$$

C. Variables

The optimization process uses the P_i converters powers as control variables. The PMS central controller imposes these optimized values by sending the updated setpoints to lower-level controllers, as in II-C. Evidently, these powers values are also related to other variables of the DC grid (e.g., fuel consumption, battery SOC), which potentially can be taken into account as well to build the objective function. Since the paper is mainly focused on fast transients, the effect of these additional variables in the optimization is not appreciable, then disregarded.

IV. Optimization Test

The test is about a variation in ship operation due to the entry maneuver in the port. At the beginning, the DC system works with the busbar connector closed, while after its opening the two buses only interact via the zones. Before the connector opening, the PMS performs a single objective optimization. After, the objective function is doubled as well, as the electrical system is divided. At this moment, the PMS starts to perform the multi-objective optimization. Once the optimization is finished, the low-level controllers are accordingly configured. All the operating conditions are in Tab. II, where the converters power is expressed both in MW and in percentage of rated size.

TABLE II. Operating conditions.

	Operating Condition							
C	OC1		OC2		OC3		OC4	
	MW	%	MW	%	MW	%	MW	%
C1	1.6	80	1.6	80	1.64	82	1.64	82
C2	1.2	80	1.2	80	1.24	83	1.24	83
C3	0.8	80	0.8	80	0.85	85	1.0	100
C4	1.2	80	1.2	80	1.25	83	1.5	100
C5	0.35	35	-0.05	5	0.12	12	0.12	12
C6	0.35	35	0.75	75	0.4	40	0.4	40
C7	2.75	92	2.75	92	3	100	3	100
C8	2.75	92	2.75	92	2.5	83	2.9	97

A. Initial condition – OC1

Before the maneuver start (i.e., OC1), the total load power is 5.5 MW, equally split between C7-C8. In this operating condition, the PMS sets the converters power outputs by (1), whereas the constraints are specified in (4)-(9). In this operating scenario, the diesel gensets are all supplying the DC grid with 80% of each rated power, while both batteries identically feed the loads with 350 kW each (i.e., equal droop setting).

B. Separated buses configuration – OC2 & OC3

When the ship starts approaching the port, the zonal distribution is split into two separated buses. This is performed by opening the busbar connector (i.e., DC switch). In the very-first seconds after this action, the ship distribution operates in a non-optimized condition (i.e., OC2). The power output of converters C1-C4 remains the same, as well as the power request from converter C7-C8. The power balance is thus guaranteed by the batteries' converters, where C5 regulates the bus 1 voltage and C6 controls the voltage on bus 2. In this unbalanced condition, C5 is devoted in charging the battery with 50 kW while C6 is able to provide 750 kW to the loads. When the system reaches steady state (after a few seconds), the PMS can calculate the new optimized power setpoints. These values are then imposed on the converters control loops. In this particular case, a two-objective optimization is performed, by working on the two functions (2)-(3), one for each single bus. All the constraints remain the same as before (5)-(9), except for the (4) equality. The latter is split into two equalities, defining the power balance on bus 1 and bus 2 as separated units. The positive outcome to reach a new optimal operating point (i.e., OC3) is enabled by the ZEDS ability in supplying the loads from both buses, while always remaining inside the capability area of interfacing converters (i.e., C5-C6). So, a portion of the load supplied by the bus 2 is now shifted to bus 1, which presents a greater generating power. Particularly, C7 converter requires 3 MW, whereas 2.5 MW are provided by C8. Both batteries now support the DGs powering.

C. Load increase – OC4

The optimization algorithm is performed every 10 min in order to check possible load variations, to keep the batteries inside the admissible SOC range. From OC3 to OC4, the load power is increased from 5.5 MW to 5.9 MW after 10 min. As C7 has already reached its rated power output, it cannot be longer exploited to shift the load to the other bus. To balance the power request, at this point the optimization algorithm can only act on the converters of bus 2, as in Table II.

V. Validation of Optmized Power management System

In this Section, the optimization test is performed as a numerical simulation in Matlab/Simulink environment. The DC ZEDS is modeled by disregarding the switching of power converters, thus adopting the Average Value Models (AVMs). Another assumption regards the voltage-controlled converters, whose current control loop is neglected. The converters control and the batteries models are defined as in [10], while a detailed description on control functionalities is in Section II-C. One remark regards the bus voltage, that is controlled by the batteries' converters. Thus, when the two buses are interconnected, the droop function results mandatory. In such a case, the PMS is in charge of coordinating the batteries converters by providing droop setpoints. The optimization is run on Matlab, which indeed implement the well-known *fmincon* for single objective task and *fminmax* for the double objective one.

A. Transient responses

In the following, simulated transients are shown to demonstrate the PMS capability in reconfiguring the system in the test scenario. The transients in Figs. 2-5 are triggered by the opening of busbar connector at t=5 s, i.e., the transition from OC1 to OC2. Indeed, at the beginning the DC grid is in the OC1 steady-state imposed by the initial optimization algorithm. Here, the four DGs operate in their optimal operating points, at 80% load factor (ratio between actual power and rated power). They supply a total power of 5.5 MW, which is equally split between the two load converters (Fig. 3). In this initial OC, the batteries regulate the bus voltage by means of equal droop coefficients, resulting in a similar power output (Fig. 4). The slight difference visible in the simulated results is mainly due to the small dissimilarity in voltage values (i.e., bus 1 VS bus 2), caused by the current flowing throughout the busbar connector and interconnection line. The effect of droop control is clear in Fig. 5, where the steady-state voltage value prior to the 5 seconds mark is lower than 1500 V. The passage from OC1 to OC2 implies opening the busbar connector is open at t=5 s. After this perturbation, the DC system moves towards a non-optimized equilibrium point (i.e., OC2). Also, when the bus is opened C1-C4 and C7-C8 keep the same steady-state power output, due to their power setpoints being not yet modified. As the two buses are now working separately, a power unbalance (i.e., excess on bus 1 and lack on bus 2) is originated, as made evident in the voltage transients of Fig. 5. To restore the buses voltages, the C5 battery converter starts absorbing power (50 kW is the final value), while C6 feeds the bus 2 reaching 750 kW power supply at t=5.4 s. As the DC microgrid is now working in a non-optimized steady-state condition (i.e., OC2), the PMS has to react to establish an optimal operation. Once defined constraints and limitations, the two-objective optimization is run to identify the power reconfiguration. The values are shown in Table II, and are imposed by the zonal controllers to ensure the optimal OC3. Evidently, the OC3 working point is reachable only in presence of a sufficient ZEDS power capability, by switching a portion of the bus 2 load to the bus 1, through zone 2 interfaces operation. To ensure the transition from OC2 to OC3, the power of C1-C4 evolve as depicted in Fig. 6. For what regard C7-C8, the power transients are in Fig. 7. Particularly, in the OC3 final condition C7 requires 3 MW (its rated power), while 2.5 MW are provided by C8. The batteries assist the bus voltage as depicted in Fig. 8.

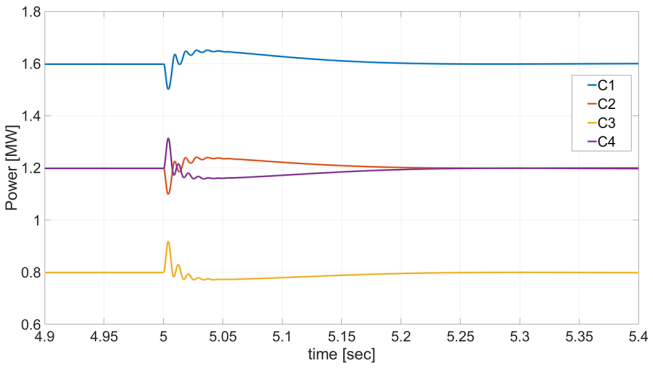

Fig. 2. Generators converters power transients, from OC1 to OC2.

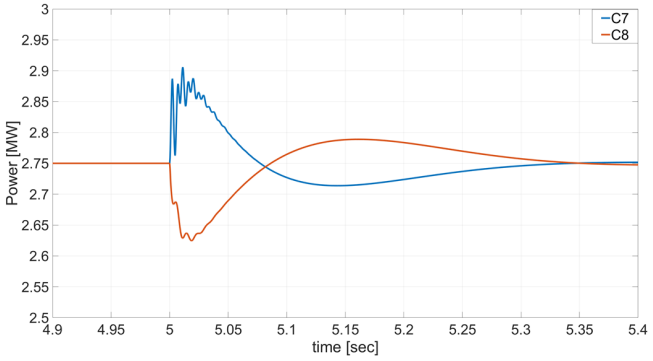

Fig. 3. Loads converters power transients, from OC1 to OC2.

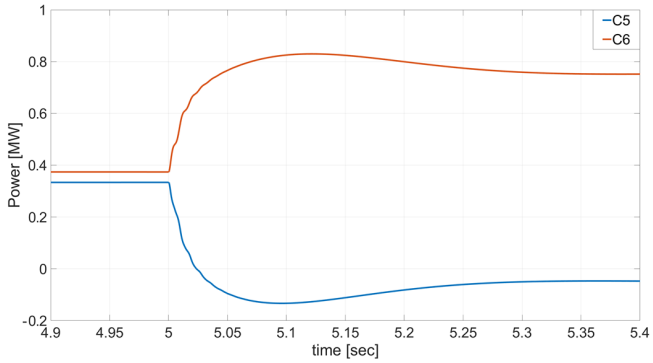

Fig. 4. Batteries converters power transients, from OC1 to OC2.

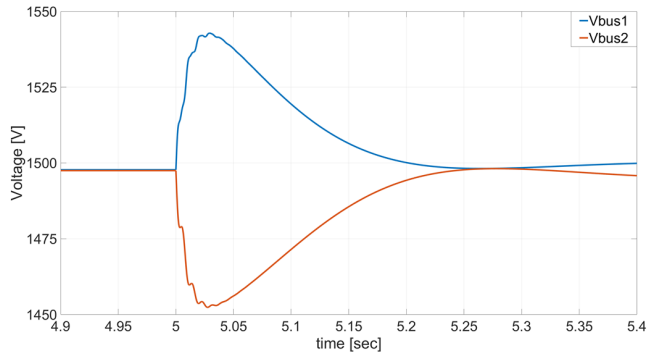

Fig. 5. Bus voltage transients, from OC1 to OC2

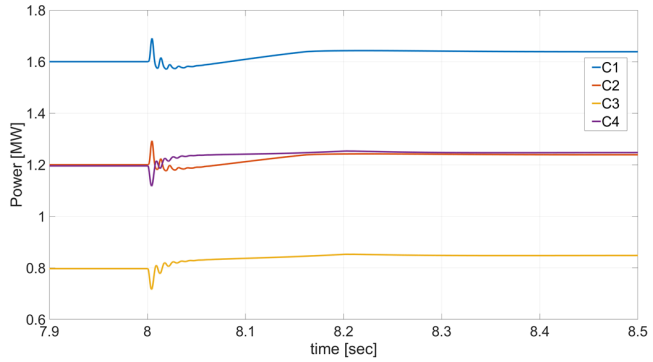

Fig. 6: Generators' converters power transients, from OC2 to OC3.

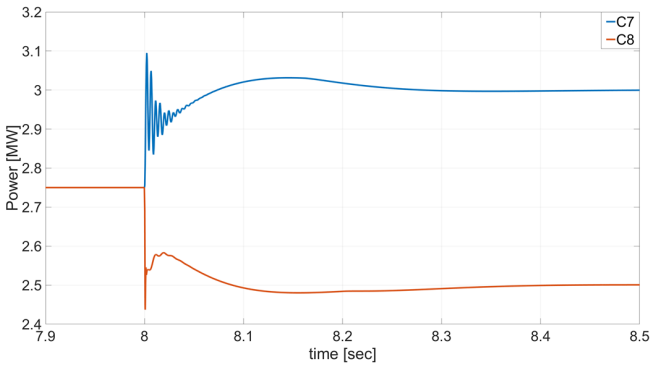

Fig. 7: Loads' converters power transients, from OC2 to OC3.

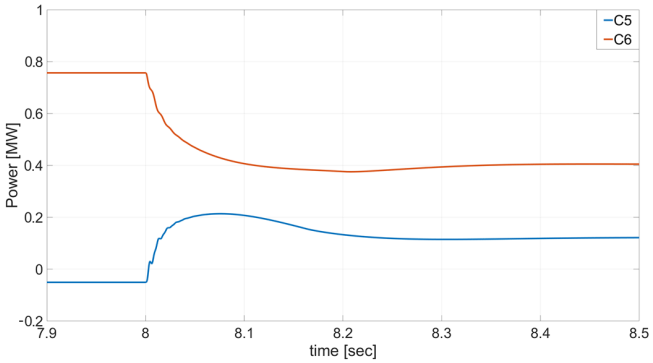

Fig. 8: Batteries' converters power transients, from OC2 to OC3.

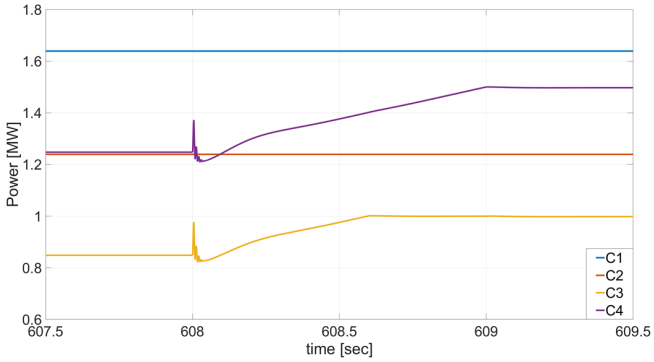

Fig. 9: Generators' converters power transients, from OC3 to OC4.

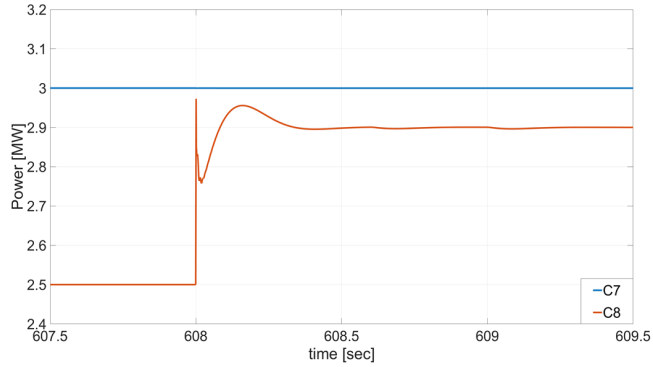

Fig. 10: Loads' converters power transients, from OC3to OC4

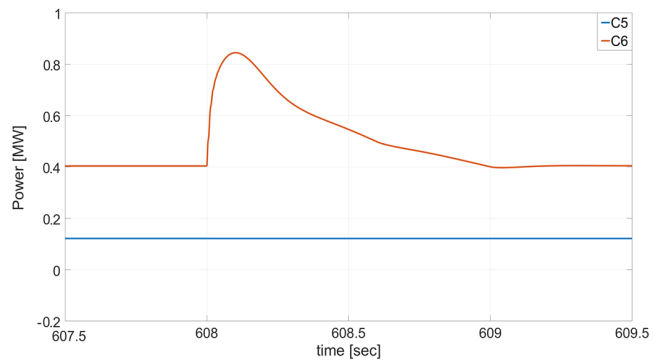

Fig. 11: Batteries' converters power transients, from OC3 to OC4.

The last transients in Figs. 9-11 are triggered by a final load increase, from 5.5 MW to 5.9 MW. The supply of this request is also optimized by the intelligent engine acting on the PMS. In particular, ten minutes after the last evolution towards OC2, the DC grid is optimally reconfigured to accept this additional load demand, while keeping the battery SOCs inside the desired ranges. To give more details on this optimization, it is firstly necessary to observe a limitation on bus 1 converter. The optimization algorithm is indeed unable to act on C7, since it has already reached its rated power of 3 MW. This means that only the setpoints on bus 2 converters are modifiable, to hold-up the power increase on C8. In particular, the output power of C3 and C4 converters are increased to match the load demand, as in Figs. 9-10. Finally, the C6 battery converter supports the bus voltage during the transient (Fig. 11), but its operating point is not modified due to the the battery output power constraint imposed by the PMS.

B. Optimized use of power converters

The four octagons of Figs. 12-15 show the outcomes of the optimization algorithm application. They represent each converter's load factor (i.e., ratio between actual and rated power). In the OC1 of Fig.12, there is an overall balance in the converters' powers. The C1-C4 converters work at 80%, while the load is equally split between C7-C8. Converters C5-C6 are also harmonized, thus providing the same power to the bus. Conversely, the OC2 in Fig. 13 is clearly unbalanced. In fact, the battery provides 75% of the C6 rated power to the grid, while C5 absorbs 5% of its rated power to charge its battery module. Then, the algorithm rebalances the system by switching the load from one bus to the other (Fig. 14). In the last OC of Fig. 15, the algorithm is no more capable of balancing the DC system, since C7 has reached its rated power and C6 has reached the limit imposed by the PMS. At this point, the only possibility is to increase the power output of DGs.

C. Optimized ship operation

The Table II OC sequence depicts a ship entering into a port. Specifically, OC1 is the navigation approaching the port, OC2 and OC3 happen when the ship is in the port area (separated bus operation ensures redundancy in such a delicate operation), and OC4 is the berthing maneuver (using thrusters). A similar OC sequence may be also applicable for a naval ship approaching combat, where normal navigation (OC1) is followed by bus separation to ensure survivability (OC2 & OC3), and subsequent weapons activation (OC4). In such situations, keeping batteries SOC in a suitable range guarantees their availability to face unexpected events, like faults or hits. At the same time, forcing DGs to work near their most efficient load factor ensures low fuel consumption, which has environmental benefits, lowers operative costs, and increases ship range.

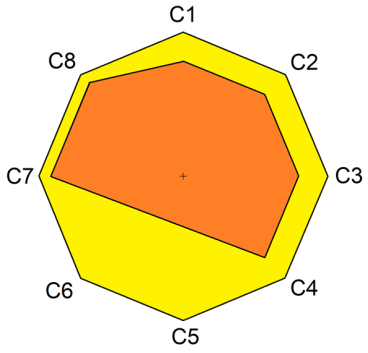

Fig. 12. Power converters load factor in OC1.

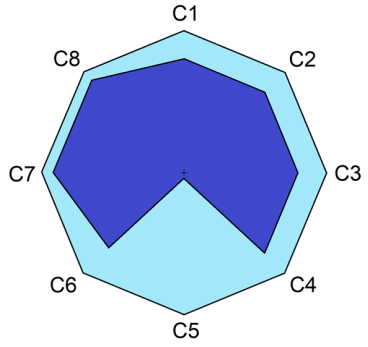

Fig. 13. Power converters load factor in OC2.

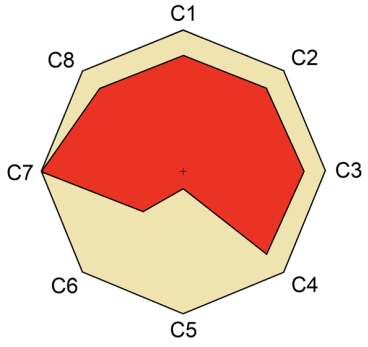

Fig. 14. Power converters load factor in OC3.

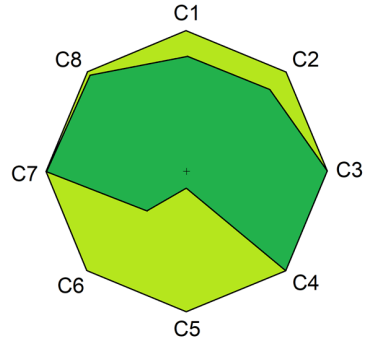

Fig. 15. Power converters load factor in OC4.

VI. Conclusions

The paper has discussed a multi-objective optimization aimed at best configuring the PMS of a zonal DC shipboard microgrid. Once imposed constraints and variables, the intelligent engine determines the best operating setpoints to be applied by the PMS, in both single and separated bus configurations. This enables high efficiency operation, while preserving the onboard batteries SOC. As a secondary goal, the best exploitation of interface converters is also ensured. Although the optimization is a multi-objective one, in this work a *minmax* strategy has been applied to obtain a single solution. In future works, a multi-objective strategy based on Game Theory (e.g., Pareto, Nash) will be applied, to identify the best possible compromise between the optimal solutions.

References

[1] S. Fang et al., "Toward Future Green Maritime Transportation: An Overview of Seaport Microgrids and All-Electric Ships," in *IEEE Trans. on Vehicular Technology*, vol. 69, no. 1, pp. 207-219, Jan. 2020.

[2] D. Bosich, M. Chiandone, G. Sulligoi, A.A. Tavagnutti, A. Vicenzutti, "High-Performance Megawatt-Scale MVDC Zonal Electrical Distribution System Based on Power Electronics Open System Interfaces," in *IEEE Trans. on Transp. Electrification,* early-access.

[3] M. U. Mutarraf et al., "Adaptive Power Management of Hierarchical Controlled Hybrid Shipboard Microgrids," in *IEEE Access*, vol. 10, pp. 21397-21411, 2022.

[4] Z. Jin, L. Meng, J. M. Guerrero and R. Han, "Hierarchical Control Design for a Shipboard Power System With DC Distribution and Energy Storage Aboard Future More-Electric Ships," in *IEEE Transactions on Industrial Informatics*, vol. 14, no. 2, pp. 703-714, Feb. 2018.

[5] "IEEE Standard for Power Electronics Open System Interfaces in Zonal Electrical Distribution Systems Rated Above 100 kW," in *IEEE Std 1826-2020 (Revision of IEEE Std 1826-2012)* , vol., no., pp.1-44, 25 Nov. 2020.

[6] P. Xie et al., "Optimization-Based Power and Energy Management System in Shipboard Microgrid: A Review," in *IEEE Systems Journal*, vol. 16, no. 1, pp. 578-590, March 2022.

[7] C.R. Petry et al., "Zonal Electrical Distribution Systems: An Affordable Architecture for the Future", *Naval Engineers Journal*, 1993, 105: 45-51.

[8] T. Ericsen, "The ship power electronic revolution: Issues and answers," *55th IEEE PCIC Technical Conference*, Cincinnati, OH, USA, 2008.

[9] S. Fang et al., "Robust Operation of Shipboard Microgrids With Multiple-Battery Energy Storage System Under Navigation Uncertainties," in *IEEE Trans. on Vehicular Techn.*, vol. 69, no. 10, pp. 10531-10544, Oct. 2020.

[10] A.A. Tavagnutti, D. Bosich and G. Sulligoi, "Strategies for Preserving the Battery SOC in DC Shipboard Power systems," *2021 IEEE Electric Ship Techn. Symposium (ESTS)*, Arlington, VA, USA, 2021, pp. 1-6.